Understanding the Physics of EHO in QH-mode on DIII-D Including the Role of Rotation Shear

Xi Chen[1], K.H. Burrell[1], N.M. Ferraro[1], T.H. Osborne[1], C.M. Muscatello[1], C.C. Petty[1], A.M. Garofalo[1], P.B. Snyder[1], R.J. Groebner[1], R. Nazikian[2], G.J. Kramer[2], B.J. Tobias[2], W.M. Solomon[2], Z. Yan[3], G.R. McKee[3], X. Ren[4], N.C. Luhmann Jr.[4], and M.E. Austin[5]

[1]*General Atomics, P.O. Box 85608, San Diego, CA 92186-5608, USA*
[2]*Princeton Plasma Physics Laboratory, P.O. Box 451, Princeton, NJ 08543-0451, USA*
[3]*University of Wisconsin-Madison, 1500 Engineering Dr., Madison, WI 53706, USA*
[4]*University of California Davis, 347 Memorial Un, Davis, CA 53706 USA*
[5]*Institute for Fusion Studies, University of Texas-Austin, Austin, TX 78712, USA*

Quiescent H-mode (QH-mode)[1] is a stationary operation mode with sustained H-mode edge pedestal and confinement but without detrimental edge-localized modes (ELMs). QH-mode operation was first discovered on DIII-D, and was subsequently seen on ASDEX Upgrade, JET, and JT-60U [2]. One of the key components of successful QH-mode operation is the edge harmonic oscillation (EHO), which opens an additional transport channel that maintains the plasma edge at conditions just below the ELM stability boundary [3]. Previous experimental and theoretical studies suggest that the EHO is the saturated state of a kink-peeling mode destabilized by edge rotation [3,4]. This paper presents linear simulations of the EHOs using the M3D-C1 MHD code [5]. The modeled mode structure agrees well with experiments and the theory of EHO being a kink-peeling mode. The rotation and rotational shear effects on the mode growth rate found in the modeling is consistent with theory and experiments. Measurements showing the EHO and the sometimes co-existing broadband MHD might be different modes are also presented.

A typical ELM-free QH-mode discharge (#157102) that is sustained until t~3500ms and accompanied by a strong steady coherent EHO on the DIII-D tokamak is modeled. The plasma is highly shaped, and slightly biased to lower single null (κ=1.9, δ=0.58, dRsep= -6mm). Starting from t=1500ms, the plasma major radius at the outer mid-plane is scanned by ±2cm at 5Hz [Fig. 1(d)] while other plasma parameters are maintained constant to improve the spatial resolution of the diagnostics that have fixed measurement locations. A suite of

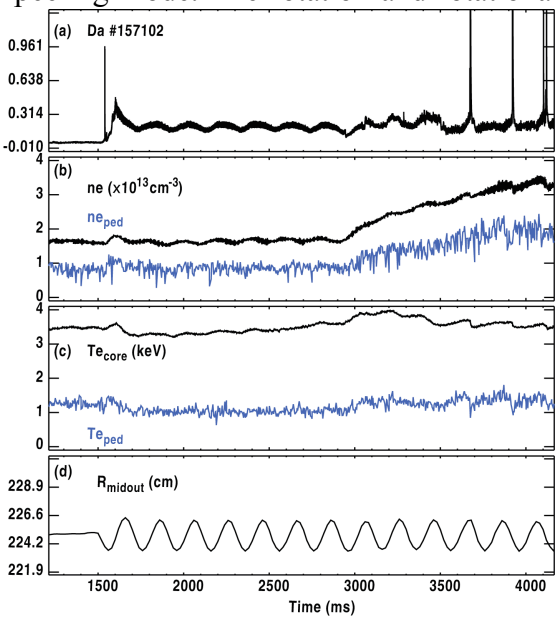

Figure 1: Time evolution of (a) Da light, (b) line-averaged and pedestal (blue) (the density rise after 3000ms is associated with the decreased NBI torque) (c) core and edge (blue) electron temperature, (d) the major radius at outer mid-plane. $|B_T| \sim 2.06$T, $|I_p| \sim 1.1$MA, $q_{95} \sim 5.4$.

pedestal diagnostics provides important data for resolving edge modes with very fine structure such as EHO. The high-resolution edge Thomson scattering system measures electron density and temperature. The edge charge exchange recombination (CER) spectroscopy system provides ion density, temperature and plasma rotation measurements by measuring carbon ions (the dominant impurity on DIII-D). A coherent EHO with an n=1 fundamental and harmonics up to n=7 is detected on edge magnetics sensors (n is the toroidal mode number). Besides the magnetics, the coherent EHO is also detected by electron cyclotron emission (ECE) radiometer, ECE-Imaging (ECE-I), beam emission spectrometer (BES) and microwave imaging reflectometer (MIR). The profile fitting is obtained by mapping data from t=2420±17.5ms onto flux surfaces using EFIT [6] equilibria reconstructed using magnetics data. Then a kinetic EFIT is generated where the bootstrap current is calculated using Sauter model [7] and neutral beam driven current is derived from a ONETWO [8] calculation.

Those profiles and equilibrium are then input into the M3D-C1 code in order to model the EHO. M3D-C1 solves the fluid equations in real 3D toroidal geometry. Linear single fluid M3D-C1 modeling with a resistive wall of n=1 to 7 modes has been conducted for the discharge in Fig. 1 at t~2420ms. Because these are linear calculations, we only compare the modeled mode structure (not the absolute amplitude) to the theory and experiments. Qualitative agreement is found in the comparison between the modeling results and various diagnostics measurements, as seen in Fig. 2. Figure 2(a) shows the modeled 2D mode structure of n=5 mode that agrees well with the ideal ELITE code [9] prediction. As shown in Fig. 2(b), the temperature fluctuation due to the n=5 mode from the modeling and from the ECE measurement both peak near ~227cm with a width of ~2.5cm. The strong density fluctuations (FWHM ~2cm, peaked at 2.5 cm inside the separatrix) associated with the modeled n=5 mode are also comparable to the BES measurements. The modeled 2D temperature and density fluctuations due to the edge mode qualitatively agree with those measured by ECE-I and MIR, respectively. The poloidal wavenumbers of n=1 to 7 derived from the M3D-C1 are consistent with those inferred from measurements at poloidally separated channels of various diagnostics, for example, for n=2, $k\theta$ (cm^{-1}) = 0.04(M3D-C1), 0.04(Magnetics), 0.03(BES), 0.03(MIR) and 0.05(ECE-I). More

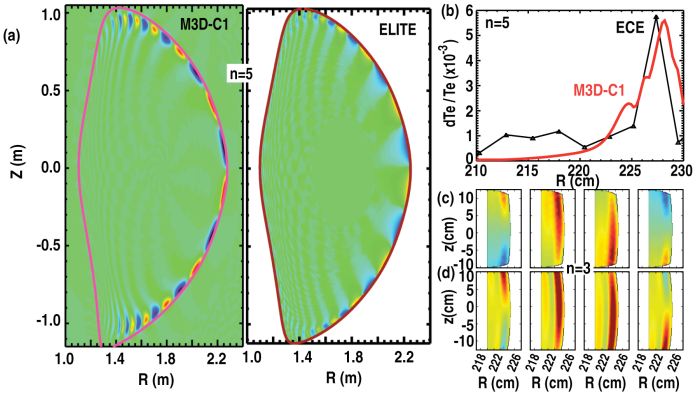

Figure 2: (a) 2D M3D-C1 pressure fluctuations (left) and ELITE predicted displacement (right) of n=5 EHO (both are without rotation); (b) Radial profile of temperature fluctuations of n=5 EHO from ECE (black) and M3DC1 (red); (c) Synthetic MIR signal with (d) M3D-C1 input of 2D density fluctuation of n=3 EHO at four different toroidal locations.

detailed comparisons with MIR measurements will be made by comparing the measurements to the synthetic MIR signal. The synthetic signal is obtained by interposing M3D-C1 modeled density fluctuations due to the EHO into a synthetic MIR diagnostic (simulating the diagnostic response), an example of which is shown in Fig. 2(c), (d) for an n=3 mode.

For a given discharge, different rotation profiles are input into the M3D-C1 code and the corresponding linear growth rates of modes in a range of toroidal mode numbers are studied. In these linear single fluid calculations, the magnitude of both the electron and ion drift velocity perpendicular to the magnetic field is the *ExB* drift, which is calculated from CER measurements. Here we modeled a QH plasma (#153440) which has a coherent EHO with dominant n=2 component near t=1725ms. In the series of modeling where the input rotation profile was scaled by 0, 25%, 50%, 75% and 100%, the linear growth rate of n=1 to n=10 modes was calculated. The mode stabilization by rotation and rotational shear occurs for all modes with n≥4. Rotation and rotational shear destabilizes the n=2 mode while barely affecting n=1 and 3 modes. The growth rates of these modes with 0% and 100% of the experimental rotation value are compared in Fig. 3 as an example. This trend is in line with previous ELITE stability calculations showing the rotational shear destabilizing low-n modes while stabilizing high-n modes [4]. The linear growth rate of n=2 increases roughly linearly with increasing rotation and rotational shear, and becomes the highest at the experimental rotation level. This is consistent with the experiment (saturated state) where n=2 EHO is dominant. Peeling-ballooning theory predicts that the EHO can exist with both signs of rotation and previous experiments have confirmed that [10]. We found consistent results in M3D-C1 modeling, that is, the linear growth rate only changes <10% when the rotation direction is reversed.

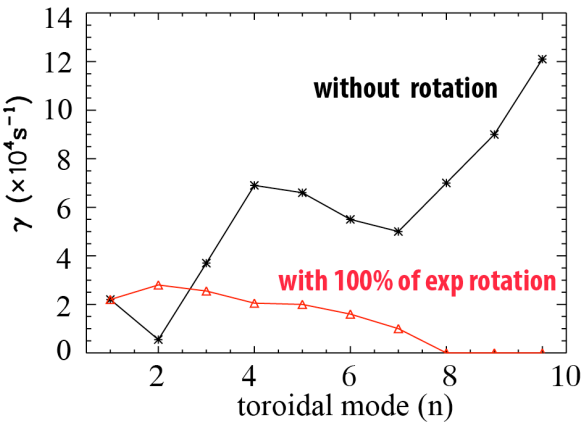

Figure 3: Linear growth rates of n=1 to 10 modes from simulations without (black) and with (red) experimental rotation.

It is often observed that some broadband MHD co-exists with the coherent EHO [Fig. 4(a), t<2700ms]. The coherent EHO rotates toroidally in the direction of plasma rotation while the broadband MHD rotates in the plasma current (Ip) direction; their poloidal phase velocities have opposite signs during counter-Ip neutral beam injection [Fig. 4(b), (c)]. The different rotation characteristics suggest they are different modes. In some highly shaped plasmas at low rotation, the coherent EHO goes away and only the broadband MHD remains [e.g., Fig. 4(a) 2700-3800ms]. These plasmas can develop a higher but wider pedestal that operates below the peeling-ballooning stability limit with good confinement. The increased

broadband fluctuations detected by BES suggest the plasma might move to a turbulence-transport dominant regime and further investigation is on going.

In summary, M3D-C1 is being applied to model the EHO in QH plasmas on DIII-D. The calculated linear eigenmode structure (~2 cm wide radially, located at the edge steep gradient region, k_θ of 0.02~0.2 cm^{-1} increasing with n) exhibits similar features as the measured EHO by magnetics, ECE, BES, ECE-I and MIR. Consistent with experiments and the initial theory, M3D-C1 modeling shows rotation and rotational shear destabilizes low-n modes while stabilizing high-n modes. Measurements show that the coherent EHO and broadband MHD have different rotation characteristics, suggesting different identities. These findings advance the physics basis for developing stationary ELM-free plasmas for ITER and beyond. However, nonlinear simulations are needed to understand the saturation mechanism for the EHO.

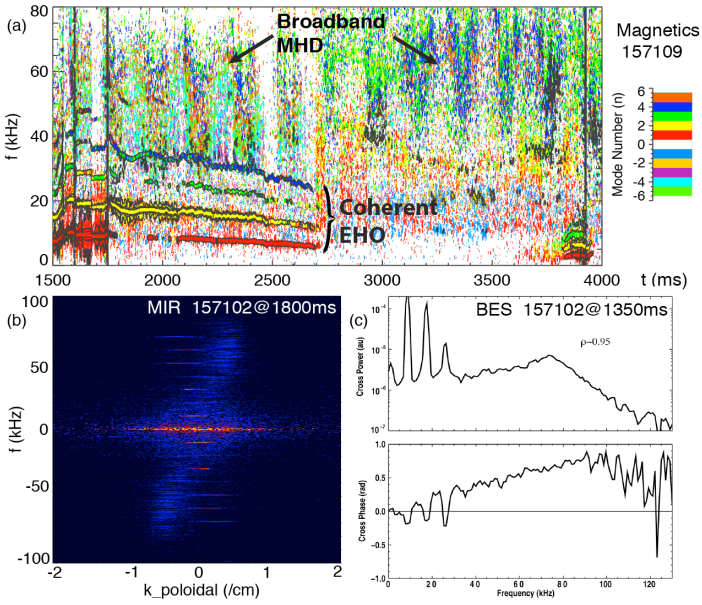

Figure 4: (a) Fourier analysis of magnetics array signals, (b) spectrogram of MIR signal (c) crosspower and phase between two poloidal BES signals of coherent EHO and broadband MHD.

This work was supported by the U.S. Department of Energy under DE-FC02-04ER5468, DE-AC02-09CH11466, DE-FG02-89ER53296, DE-FG02-99ER54531, and DE-FG03-97ER54415.

[1] K.H. Burrell, et al., Bull. Am. Phys. Soc. 44, 127 (1999)
[2] W. Suttrop, et al., Plasma Phys. Controlled Fusion 45, 1399 (2003); W. Suttrop, et al., Nucl. Fusion 45, 721 (2005); Y. Sakamoto, et al., Plasma Phys. Controlled Fusion 46, A299 (2004); N. Oyama, et al., Nucl. Fusion 45, 871 (2005)
[3] T.H. Osborne, et al., J. of Phys. 123, 012014(2008); K.H. Burrell, et al., Nucl. Fusion 49, 085024 (2009)
[4] P.B. Snyder, et al., Nucl. Fusion 49, 961 (2007); A.M. Garofalo, et al., Phys. Plasmas 22, 056116 (2015)
[5] N.M. Ferraro, S.C. Jardin, J. Comp. Phys. 228, 7742 (2009)
[6] L.L. Lao, et al., Nucl. Fusion 25, 1611 (1985)
[7] O. Sauter, C. Angioni and Y.R. Lin-Liu, Phys. Plasmas 9, 5140 (2002)
[8] R.J. Goldston, et al., J. Comp. Phys. 43, 61 (1981)
[9] P.B. Snyder, H.R. Wilson, et al., Phys. Plasmas 9, 2037 (2002).
[10] K.H. Burrell, et al., Phys. Rev. Lett. 102, 155003 (2009)